Andesite and dacite genesis via contrasting processes: the geology and geochemistry of El Valle Volcano, Panama

Marc J. Defant[1], Lee F. Clark[1], Robert H. Stewart[1], Mark S. Drummond[2], Jelle Z. de Boer[3], René C. Maury[4], Hervé Bellon[5], Thomas E. Jackson[1], and Juan F. Restrepo[1]

[1] Department of Geology, University of South Florida, Tampa, FL 33620, USA
[2] Department of Geology, University of Alabama at Birmingham, Birmingham, AL 35294, USA
[3] Department of Earth and Environmental Sciences, Wesleyan University, Middletown, CT 06457, USA
[4] Laboratoire de Pétrologie et UA 1278, Université de Bretagne Occidentale, 29287 Brest, France
[5] Laboratoire de Géochimie et de Géochronologie et UA 1278, Université de Bretagne Occidentale, 29287 Brest, France

Abstract. The easternmost stratovolcano along the Central American arc is El Valle volcano, Panama. Several andesitic and dacitic lava flows, which range in age 5–10 Ma, are termed the old group. After a long period of quiescence (approximately 3.4 Ma), volcanic activity resumed approximately 1.55 Ma with the emplacement of dacitic domes and the deposition of dacitic pyroclastic flows 0.9–0.2 Ma. These are referred to as the young group. All of the samples analyzed are calc-alkaline andesites and dacites. The mineralogy of the two groups is distinct; two pyroxenes occur in the old-group rocks but are commonly absent in the young group. In contrast, amphibole has been found only in the young-group samples. Several disequilibrium features have been observed in the minerals (e.g., oscillatory zoning within clinopyroxenes). These disequilibrium textures appear to be more prevalent among the old- as compared with the young-group samples and are most likely the result of magma-mixing, assimilation, and/or polybaric crystallization. Mass-balance fractionation models for major and trace elements were successful in relating samples from the old group but failed to show a relationship among the young-group rocks or between the old- and young-group volcanics. We believe that the old-group volcanics were derived through differentiation processes from basaltic magmas generated within the mantle-wedge. The young group, however, does not appear to be related to more primitive magmas by differentiation. The young-group samples cannot be related by fractionation including realistic amounts of amphibole. Distinctive geochemical features of the young group, including La/Yb ratios > 15, Yb < 1, Sr/Y > 150, and Y < 6, suggest that these rocks were derived from the partial melting of the subducted lithosphere. These characteristics can be explained by the partial melting of a source with residual garnet and amphibole. Dacitic material with the geochemical characteristics of subducted-lithosphere melting is generated apparently only where relatively hot crust is subducted, based on recent work. The young dacite-genesis at El Valle volcano is related to the subduction of relatively hot lithosphere.

Introduction

It has become apparent from both experimental and geochemical studies that most orogenic andesites and dacites are derived from basaltic magmas through differentiation processes such as crystal fractionation, assimilation, mixing, etc. Recently, Drummond and Defant (in press) and Defant and Drummond (in press) showed that some dacites and andesites in recent-arc environments are derived directly from the partial melting of the subducted lithosphere. These cases exist where young and relatively hot oceanic crust is subducting. El Valle volcano is unique in that apparently it displays two distinct periods of andesitic and dacitic volcanism derived from contrasting petrogenetic processes.

De Boer et. al. (1988) documented recent calc-alkaline volcanic activity throughout Panama, a region previously thought to be void of extensive Quaternary volcanism. The volcanoes extend approximately 350 km from the Costa Rican border to central Panama (El Valle, Fig. 1). These are new developments considering that as recently as 1987, Okaya and Ben-Avraham stated that "Volcanism is not active at present" in Panama (we have detected 300-year-old lava flows at La Yeguada volcano). De Boer et. al. (1988) proposed the existence of aseismic, oblique subduction below western Panama. Heil (1988) and Silver et. al. (1990) independently documented the presence of recent structures in the accretionary prism suggesting oblique subduction along the
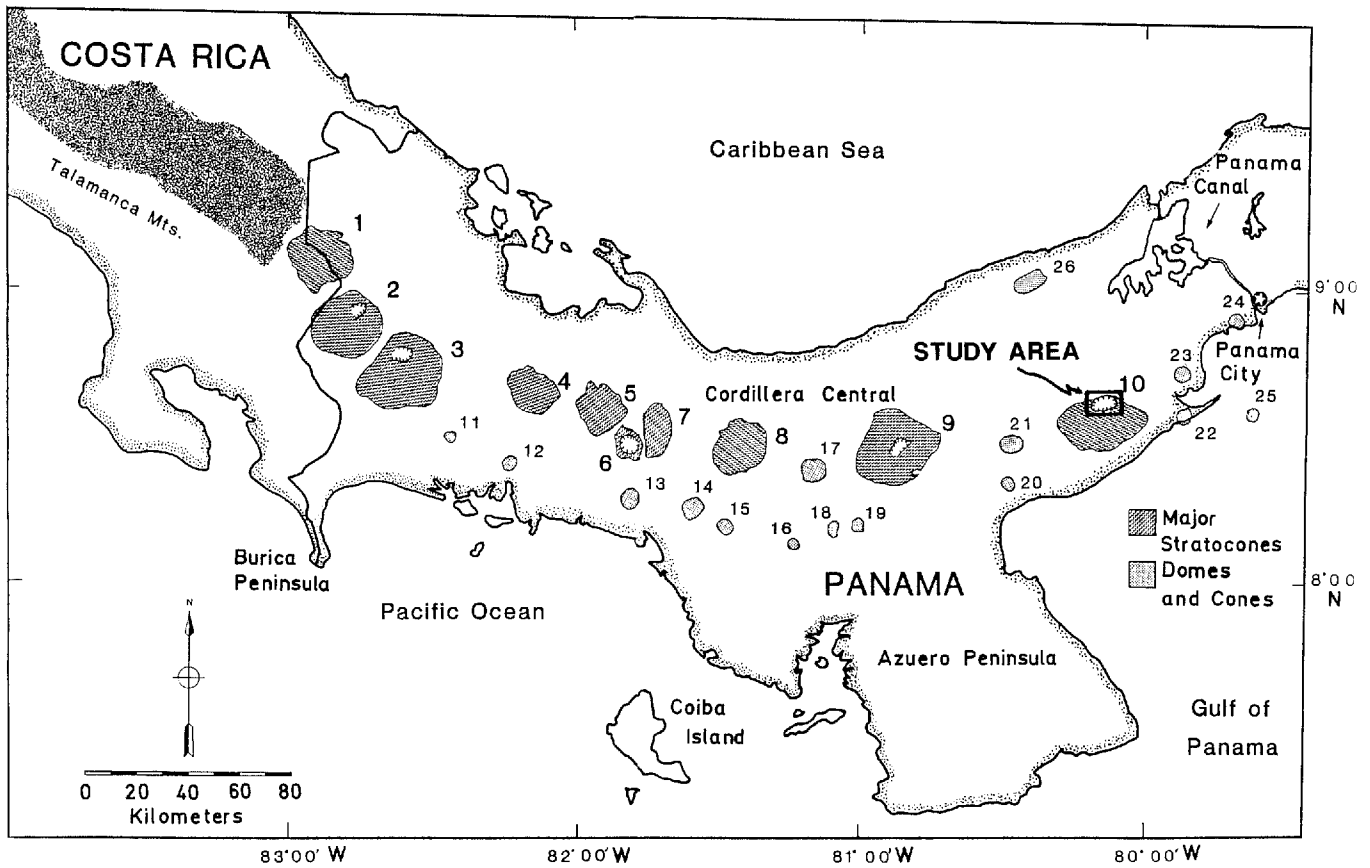
Fig. 1. Major volcanic centers of the Quaternary volcanic arc of western Panama: *1* Cerro Fabrega; *2* Tisingal (Cerro Pecon); *3* El Baru; *4* Cerro Chorcha; *5* Cerro Fonseca; *6* Cerro Colorado; *7* Cerro Santiago; *8* Cerro Buenos Aires; *9* La Yeguada complex; *10* El Valle. Smaller domes and cones: *11* Algarrobos; *12* Gran Galera de Chorcha; *13* Cerro San Felix; *14* Cerro Viejo; *15* Cerro Guayabal; *16* Cerro La Petra; *17* Cerro Canaxa; *18* Cerro San Francisco; *19* Laguna del Pato; *20* Cerro Cana de Nata; *21* Cerro Guacamaya; *22* Cerro Chame; *23* Cerro Cermeno; *24* Cerro Cabre; *25* Bono-Otoque Islands; *26* Cerro San Miguel de la Borda. The study area is outlined
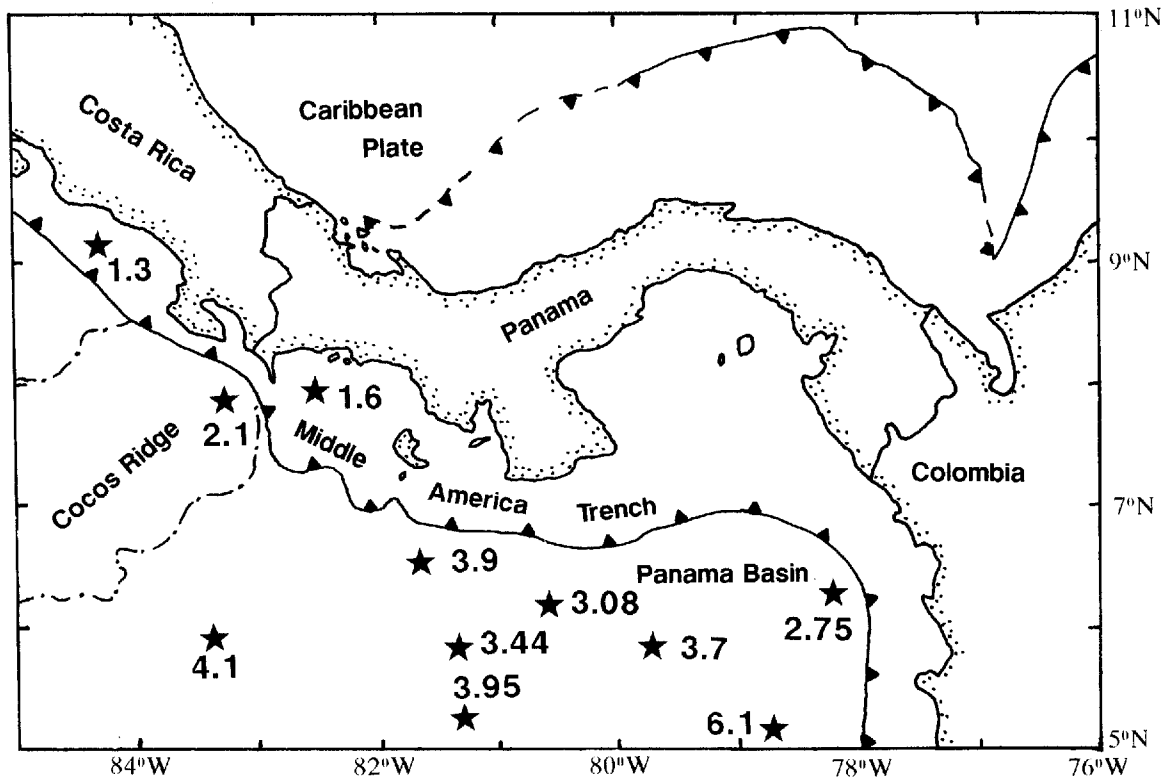

Fig. 2. Regional tectonic setting of Panama (after Heil 1988; de Boer et. al. 1988). Selected heat-flow units (*stars*) (from Bowin 1976)

Legend:

- Qf — Fan deposits
- Qls — Lake sediments
- Qid — India Dormida ignimbrite
- Qvd — Dacitic domes
- Qeh — El Hato dacitic pyroclastic flows
- Tpc — Piedra coarse-grained andesitic flow
- Tpf — Piedra fine-grained andesitic flow
- Tia — Iguana pyroclastic flows
- Tra — Rio Anton pyroclastic flows
- Tgd — Guacamayo dacitic flow

—— — — Contact
Dashed where approximately located

—— — — ·· Fault
Dashed where approximately located; dotted where concealed

●●● Inferred position of ring fracture (caldera fault)

(Crater

▲ Sample location ★ Summit of dome
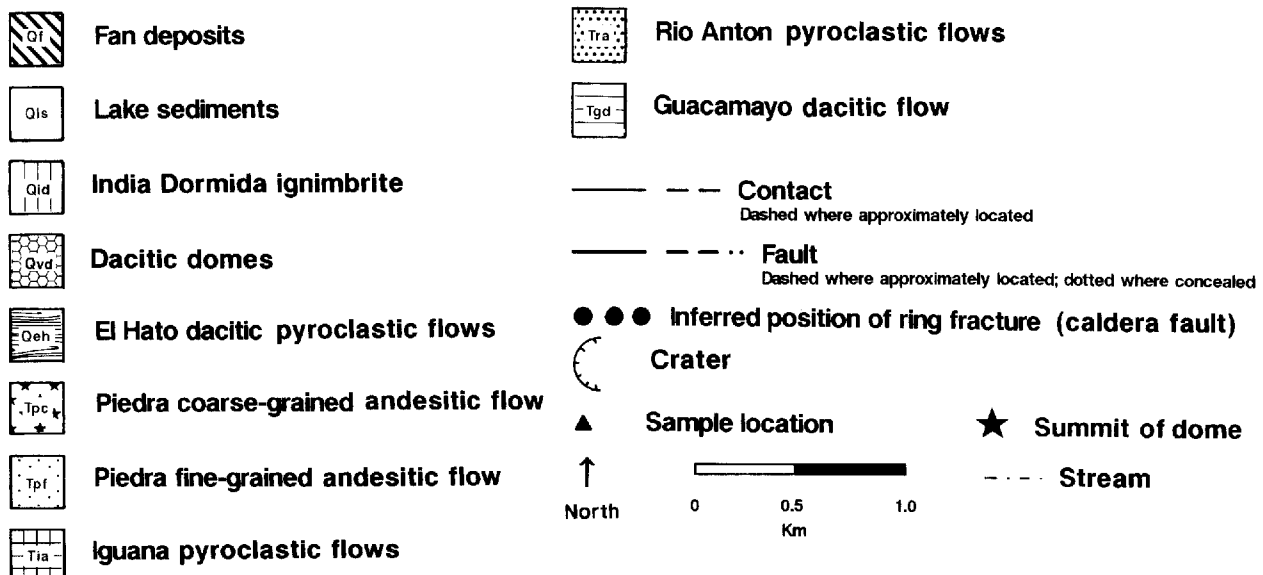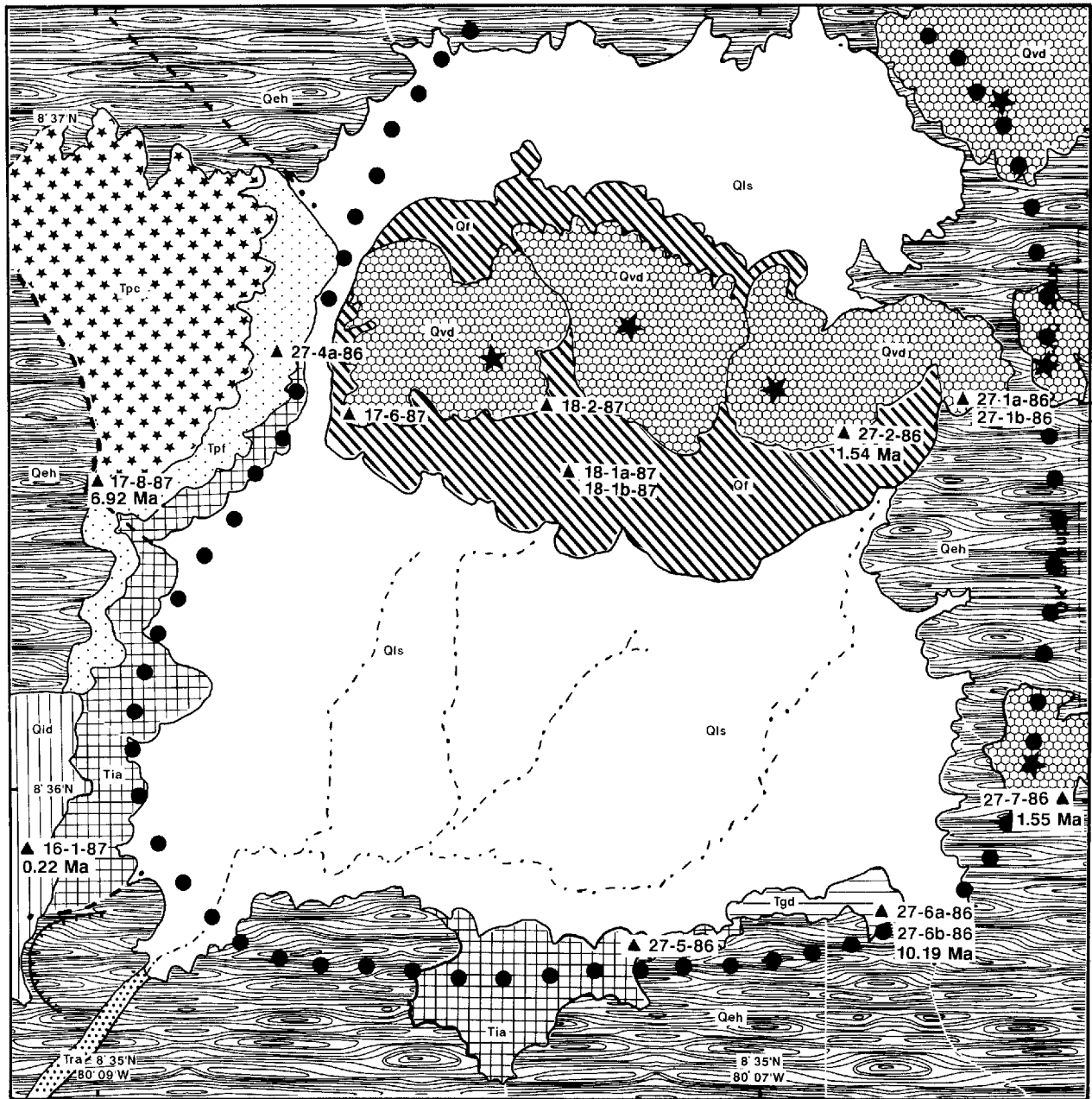
↑ North   0   0.5   1.0 Km

- · - Stream

Fig. 3. Geologic map of El Valle volcano showing geologic units, sample locations, and inferred position of caldera rim fault (after Clark 1989)

Table 1. Major and trace element analyses and K-Ar radiometric dates for the young and old groups and corresponding xenoliths

	16-1-87	17-6-87	27-7-86	27-1a-86	27-1b-86	27-2-86	18-2-87
SiO_2	65.50	66.23	67.13	68.18	58.61	68.71	66.80
TiO_2	0.26	0.25	0.26	0.28	0.60	0.24	0.21
Al_2O_3	17.60	17.20	17.49	17.81	17.48	17.37	17.50
Fe_2O_3[a]	2.78	2.60	3.02	2.80	6.93	2.32	1.96
MnO	0.08	0.08	0.09	0.06	0.12	0.07	0.05
MgO	1.12	1.13	0.25	0.95	3.59	0.97	0.79
CaO	4.43	4.40	4.88	4.10	7.44	3.86	4.41
Na_2O	4.33	4.24	4.15	4.29	3.71	4.31	4.75
K_2O	1.25	1.29	1.14	1.53	1.67	1.70	1.48
P_2O_5	0.12	0.12	0.13	0.10	0.21	0.10	0.10
H_2O^+	1.36	1.34	0.02	0.21	0.42	0.50	0.75
H_2O^-	0.67	0.82	0.75	0.32	0.19	0.62	0.50
Total	99.50	99.70	99.31	101.63	100.97	100.77	99.30
K-Ar dates	0.22 ($\pm$0.07)	–	1.55 ($\pm$0.25)	–	–	1.54 ($\pm$0.23)	–
Cr	6	5	4	5	6	10	8
Ni	8	8	5	8	9	7	4
Rb	23	24	22	24	25	22	21
Sr	707	681	705	811	800	772	841
Y	2	3	4	2	5	2	2
Zr	62	63	54	71	67	71	66
Nb	6	7	8	3	5	7	8
Ba	650	626	601	760	720	752	578
Th	–	–	0.7	2.9	2.9	–	–
U	–	–	0.3	1.3	1.1	–	–
La	–	–	9.1	9.5	9.7	–	–
Ce	–	–	16.5	17.7	18.6	–	–
Nd	–	–	9.4	9.3	9.6	–	–
Sm	–	–	1.2	1.4	1.7	–	–
Eu	–	–	0.64	0.56	0.57	–	–
Yb	–	–	0.5	0.6	0.5	–	–
Lu	–	–	0.05	0.05	0.06	–	–
Group	YG	YG	YG	YG	YG	YG	YG

southeastern extension of the Middle America Trench south of Panama. Traditionally, motion between the Caribbean and Nazca plates in this region has been ascribed to an east-west left-lateral transform fault which developed along the "former trench" (Jordan 1975; Lonsdale and Klitgord 1978; Okaya and Ben-Avraham 1987; Adamek et. al. 1988; Munoz 1988).

The extension of the Central American arc in western Panama consists of ten major stratovolcanoes. Approximately 15–20 domes and cones parallel the main arc to the south (Fig. 1). A geochemical and geological reconnaissance study of the arc was conducted by Restrepo (1987), Defant et. al. (1987), and de Boer et. al. (1988). These studies focused primarily on along-arc geochemical variations and relationships between tectonics and geochemistry. Mapping and analytical work at specific volcanoes in western Panama was initiated in an attempt to document the evolution of this segment of the Central American arc (Clark 1989; Jackson 1990; Richerson 1990). The objectives of this research are to: (1) document the eruptive history of El Valle volcano; (2) investigate the petrogenetic evolution of the volcano including the source of magma generation; (3) relate this volcanic activity to a regional tectonic model.

Geologic setting and volcanic stratigraphy

The lack of a well-defined Benioff zone below Panama is the probable result of subduction of relatively hot oceanic lithosphere (de Boer et. al. 1988). Heat-flow values through the Panama basin average 3.44 HFU (heat-flow units) (Von Herzen and Anderson 1972; Bowin 1976) (Fig. 2). This value is almost three times the average heat-flow value of the Caribbean (1.3 HFU – Epp et. al. 1970). De Boer et. al. (1988) suggested that the high heat-flow in the Panama basin might be due to the thinning of the crust.

El Valle volcano is located at the easternmost extent of the Central American volcanic chain (Fig. 1). The summit of the volcano contains a 20 km^2 caldera. The base of the mountain is underlain by mid-Miocene ignimbritic deposits that extend southward to the Pacific coast. A sequence of 5- to 10-Ma (IRHE 1985) volcanic deposits composed of the Piedra coarse- and fine-grained andesitic flows, the Guacamayo dacitic flow, and the Rio Anton and Iguana pyroclastic flows (Fig. 3), are believed to overlie the ignimbrites directly. An age of 6.92 Ma has been obtained from an andesitic lava flow (the Piedra coarse-grained andesitic flow) from the northwest section of the caldera-wall (Fig. 3). An approximately 3.4-Ma period of inactivity followed the Pliocene eruption of the Piedra coarse-grained andesitic flow. Volcanic activity resumed at approximately 1.55 Ma with the emplacement of dacitic domes (Fig. 3). Proximal pyroclastic eruptions 1.33 Ma led to the deposition of the El Hato pyroclastic flows (IRHE 1985) – an extensive unit that covers most of the flanks of the volcano and may have corresponded with the collapse of the caldera. This was followed

312

Table 1 (continued)

	18-1a-87	18-1b-87	27-5-86	27-6a-86	27-6b-86	17-8-87	27-4a-86
SiO_2	49.60	49.20	56.46	67.30	66.86	58.50	58.17
TiO_2	0.94	0.57	0.69	0.56	0.59	0.52	0.60
Al_2O_3	17.50	21.80	17.07	15.50	15.63	16.70	17.56
Fe_2O_3 [a]	10.90	9.04	7.23	2.71	4.02	5.66	6.36
MnO	0.35	0.19	0.11	0.04	0.11	0.11	0.13
MgO	6.20	3.44	3.72	0.79	1.35	3.31	3.75
CaO	8.36	8.30	7.56	3.89	3.94	6.83	7.94
Na_2O	3.31	3.97	3.68	4.49	4.15	3.35	3.25
K_2O	0.50	0.43	1.03	2.23	2.10	1.13	0.67
P_2O_5	0.15	0.39	0.33	0.17	0.18	0.20	0.18
H_2O^+	1.00	1.36	0.89	0.67	0.36	1.32	0.80
H_2O^-	0.65	0.90	1.16	0.62	0.82	0.70	0.87
Total	99.46	99.59	99.93	98.97	100.11	98.33	100.28
K-Ar dates	–	–	–	–	10.19 ($\pm$0.37)	6.92 ($\pm$0.53)	–
Cr	125	20	33	9	9	44	28
Ni	43	18	37	8	8	30	31
Rb	11	9	23	47	46	14	20
Sr	579	772	683	370	355	499	472
Y	31	14	13	29	20	12	14
Zr	34	44	66	150	145	78	68
Nb	5	6	8	11	11	7	7
Ba	386	400	511	999	862	658	720
Th	0.6	–	1.8	–	2.7	1.5	0.9
U	0.4	–	0.8	–	1.2	0.7	0.4
La	8.7	–	17.7	–	17.2	13.2	8.7
Ce	23.6	–	29.4	–	31.8	23.6	16.6
Nd	19.1	–	16.5	–	15.9	13.3	11.1
Sm	4.8	–	2.8	–	3.4	2.2	2.2
Eu	1.48	–	1.05	–	1.03	0.8	0.77
Yb	2.8	–	1.6	–	2.2	1.5	1.4
Lu	0.34	–	0.2	–	0.29	0.26	0.2
Group	X	X	OG	OG	OG	OG	OG

[a] Total Fe as Fe_2O_3. All major elements (wt.%) determined by XRF (from Restrepo 1987) (see Clark 1989, for details concerning precision and accuracy on major and trace elements). All elements determined by ICP/MS and XRF and reported as ppm (from Clark 1989). Age calculations carried out using constants from Steiger and Jager (1977). OG = old-group samples (5–10 Ma); YG = young-group samples (<1.55 Ma); X = Xenoliths

by the extrusion of more domes along an east-west lineament inside the caldera and along the caldera-rim 0.9–0.2 Ma (Fig. 3) (IRHE 1985). The easternmost dome in the caldera is heterogeneous (dominantly dacitic with subordinate andesite). The central dome in the caldera contains gabbroic xenoliths.

More than 90 m of sediments were deposited in a lake formed after caldera-collapse which later drained through a breach in the southwest caldera-wall. We have obtained an age of 0.22 Ma from the India Dormida dacitic ignimbrite, presumably originating from a well-preserved crater located on the southwest rim of the caldera (Fig. 3).

Results

Major and trace element geochemistry

The El Valle major-, trace-. and REE (rare-earth-element)-data and K-Ar radiometric dates are presented in Table 1. All of the lavas are either andesites or dacites based on the nomenclature of Peccerillo and Taylor (1976). These samples have been subdivided on the basis of stratigraphy and K-Ar dates into two categories: the old- (5–10 Ma) and young-group andesites and dacites (approximately 1.55–0.22 Ma).

The young and old groups and two xenoliths collected from the central dacitic dome in the caldera do not fall consistently along similar variation trends (Figs. 4, 5). The dacites from the young group have distinctly higher concentrations in Sr but lower abundances in the other incompatible elements (e.g. Ba, Zr, Rb, Nb, and particularly Y) compared with the old-group dacites. The young-group andesite has lower Y, Cr, Nb, and Ni, and higher K_2O, Sr, Th, and U than the old-group andesites.

All of the samples exhibit calc-alkaline characteristics (Restrepo 1987; Clark et. al. 1988) and accordingly fall within calc-alkaline fields on most discrimination diagrams. They are plagioclase phyric, quartz and hypersthene normative, display high ratios of large-ion lithophile elements (LILE) to high-field-strength elements (HFSE), and low TiO_2 concentrations, all typical of calc-alkaline volcanics.
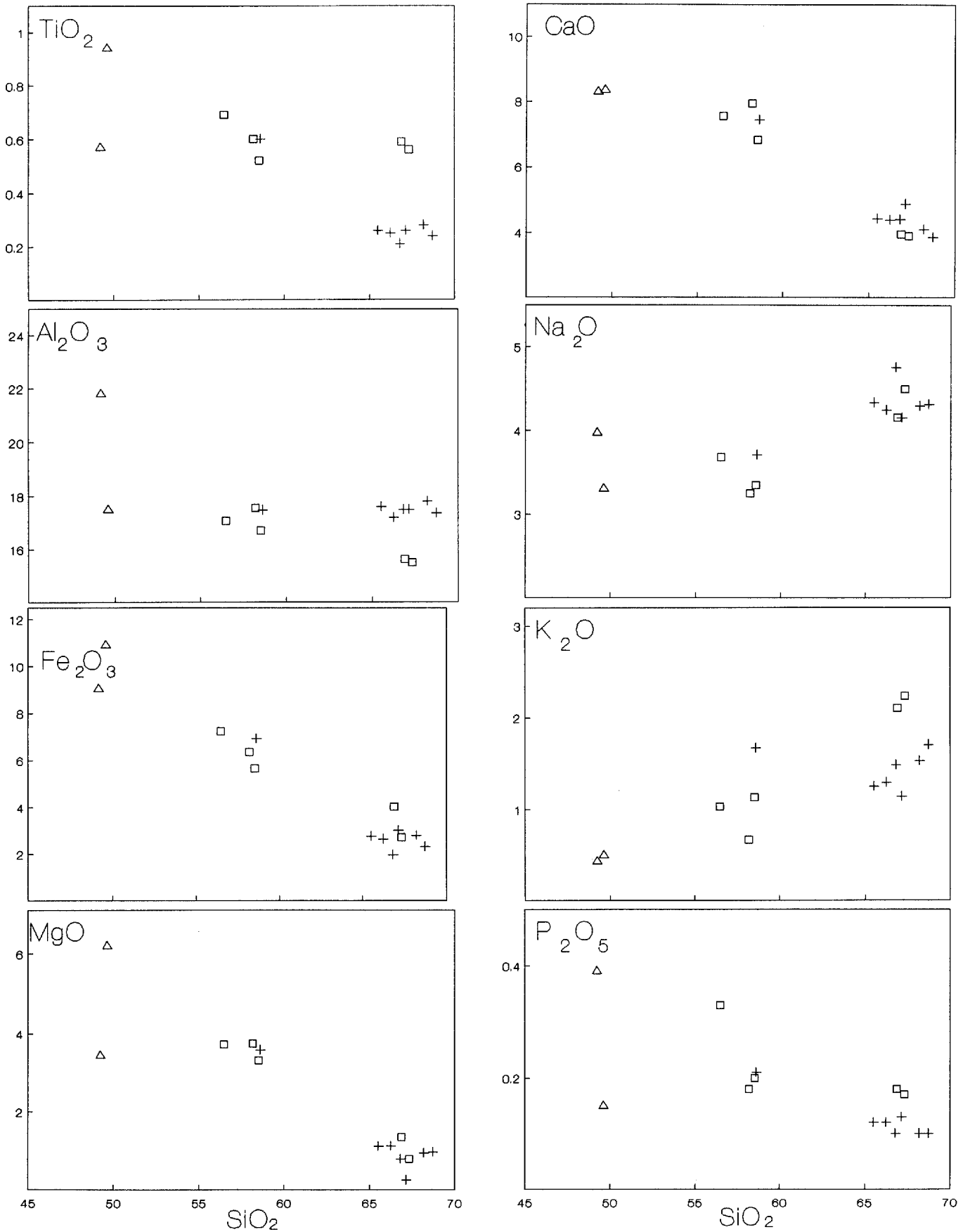
Fig. 4. Major-element (wt.%) variation diagrams. *Triangles* = gabbroic xenoliths found in young dacitic dome samples. *Squares* = old-group (5–10 Ma) and *crosses* = young-group andesites and dacites (< 1.55 Ma)
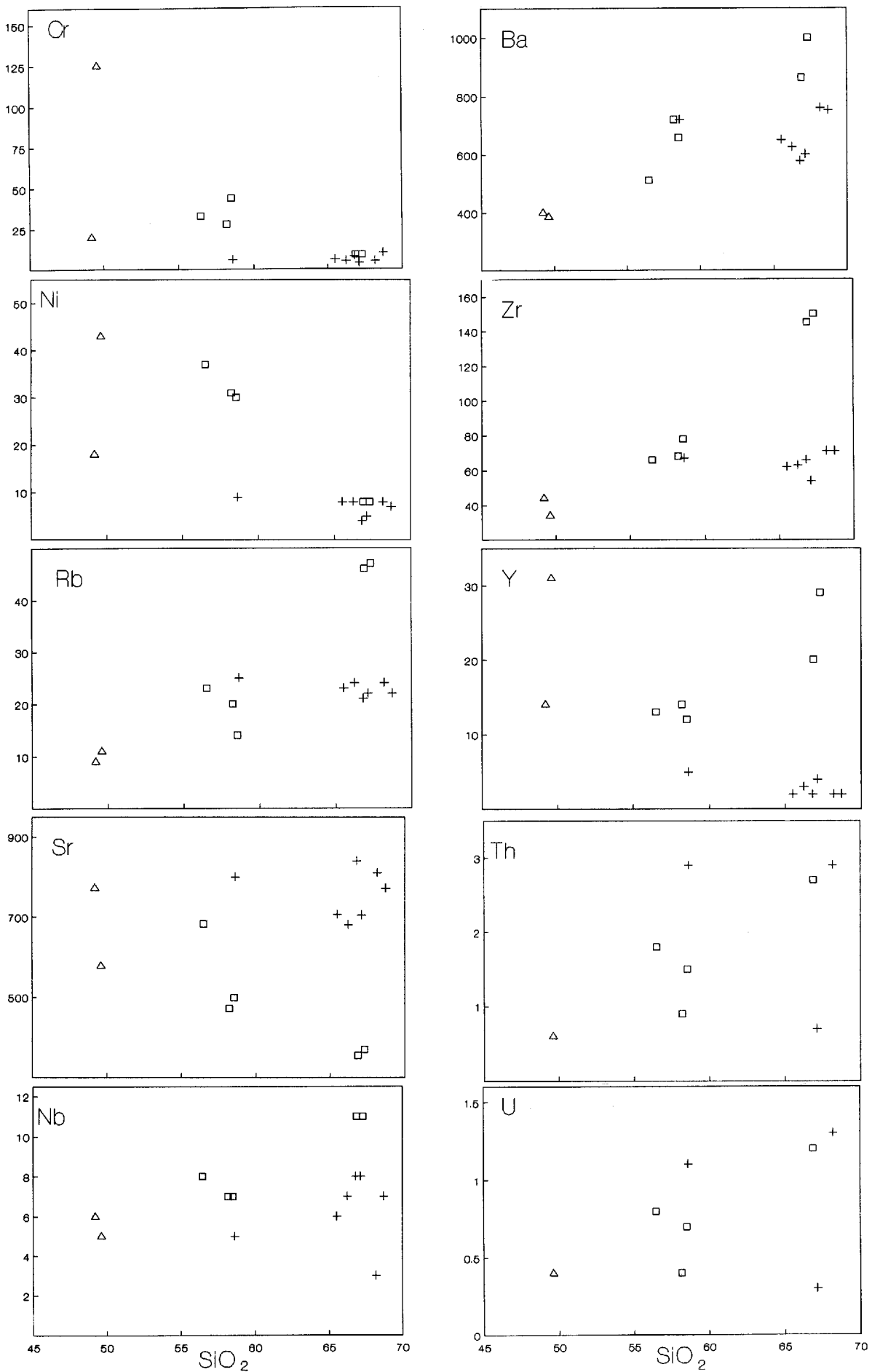
Fig. 5. Trace-element (ppm) variation diagrams. Symbols are defined in Fig. 4

Isotope geochemistry

$^{87}Sr/^{86}Sr$ and $^{143}Nd/^{144}Nd$ ratios have been determined for six samples (Table 2). The range in both Sr and Nd isotopic ratios is small (0.703500–0703740, 0.512890–0.513054, respectively). The El Valle data fall well within the mantle array and are comparable to those island arcs with the least radiogenic Sr and most radiogenic Nd isotopic ratios (isotopically coherent group, $^{87}Sr/^{86}Sr < 0.704$, of White and Patchett 1984) (Fig. 6). The El Valle samples have some of the lowest Sr isotopic ratios determined from the Central American arc, and most importantly there is no significant isotopic difference between the young and old groups.

Mineralogy and petrology

All of the samples are porphyritic and a few of the andesites display trachytic textures. All the thin-sections contain groundmass glass. Alteration of amphibole to opacite is present, and other alteration

products are minor. Glomeroporphyritic inclusions are observed only in the old-group andesites.

Pyroxene. Representative clinopyroxene and orthopyroxene analyses are presented in Table 3. The earliest-formed silicate phase appears to be clinopyroxene. Clinopyroxene is found only in old-group samples, and orthopyroxene is common in the old group but exists in trace amounts in the young-group andesite. With the exception of the small amount of pigeonite found in one sample, the pyroxenes are typical of the calc-alkaline series. The orthopyroxenes are either bronzites or hyperstenes ($Mg\%_{65-77}$), and the clinopyroxenes all possess evolved augitic compositions with $Ca\%_{36-42}$ and $Mg\%_{38-48}$ ranges. The clinopyroxenes display oscillatory zoning from core to rim indicative of disequilibrium.

Plagioclase. Representative plagioclase compositions are given in Table 3. Plagioclase is the dominant phenocryst phase. Almost all of the plagioclase phenocrysts display complex zoning including normal, reverse, oscillatory, and sometimes discontinuous zoning. The plagioclase phenocrysts are embayed, resorbed, anhedral to euhedral, and vary considerably in the extent of glass inclusions. Sieve-textures are more commonly observed in the old- compared with the young-group plagioclases.

Table 2. $^{87}Sr/^{86}Sr$ and $^{143}Nd/^{144}Nd$ ratios from El Valle samples

Old group	17-8-87	27-4a-86	27-5-86	27-6b-86
$^{87}Sr/^{86}Sr$	0.70366 ± 1 [a]	0.70350 ± 1 [a]	0.703635 ± 6 [b]	0.703740 ± 12 [b]
$^{143}Nd/^{144}Nd$	0.51296 ± 1 [a]	0.51297 ± 1 [a] (0.51298 ± 1) [a]	0.512954 ± 11 [b]	0.513054 ± 11 [b]

Young group	27-1b-86	27-1a-86
$^{87}Sr/^{86}Sr$	0.703740 ± 35 [b]	0.703536 ± 16 [b]
$^{143}Nd/^{144}Nd$	0.51289 ± 2 [a]	0.512934 ± 14 [b]

Sr and Nd isotopic data reported as measured. [a] Samples analyzed at University of Florida. The measured value for La Jolla standard Nd is 0.51185 ± 1 based on a running average over a four year period. The measured value for NBS SRM987 is 0.71023 ± 1. [b] Samples analyzed at Rutgers University, New Brunswick. The measured values for Eimer and Amend Sr and NBS SRM987 Sr are 0.708000 and 0.710251, respectively. The measured value for La Jolla standard (2 sigmar error) of Sr and Nd isotopes is as given. External precision, estimated from replicate runs of standards, is ± 0.000030 for both Sr and Nd isotopes
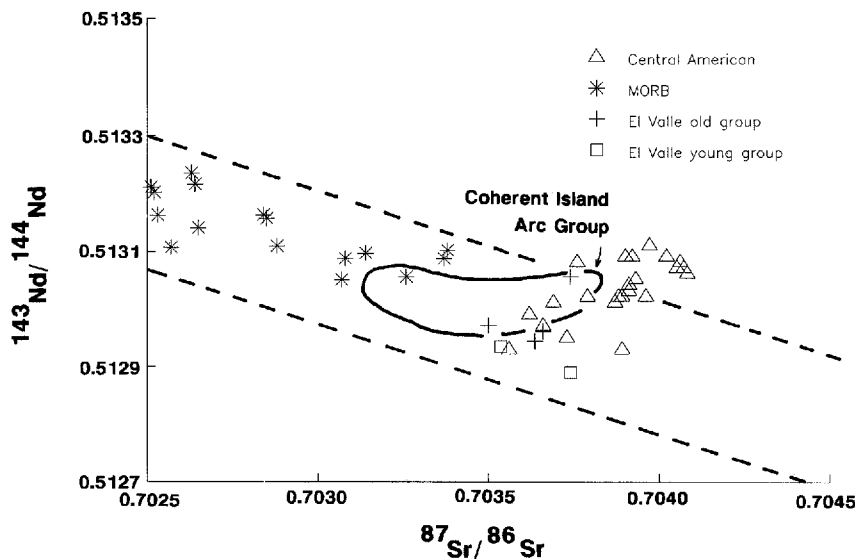

Fig. 6. $^{87}Sr/^{86}Sr$ vs. $^{143}Nd/^{144}Nd$. Data from MORB are from White and Hofmann (1982) and Central American arc from Feigenson and Carr (1987). The mantle array is approximated from MORB and OIB (ocean-island basalt) data (White and Hofmann 1982). Coherent island-arc field is taken from data from White and Patchett (1984) representing the Marianas, Izu, Aleutian, and New Britain arcs

Table 3. Selected phenocryst and microphenocryst analyses

	17-8.2	17-8.6	27-4a.1	27-5.4	27-6b.3	17-8.2	17-8.3	17-8.4	27-7.3
SiO_2	52.26	51.76	50.10	53.83	53.19	44.96	45.24	45.19	54.79
TiO_2	0.12	0.26	0.97	0.20	0.19	–	–	–	–
Al_2O_3	0.84	1.91	4.26	1.53	1.11	34.57	33.77	34.49	28.06
Cr_2O_3	0.00	0.00	0.29	0.00	0.00	–	–	–	–
FeO^a	22.54	10.91	10.42	15.63	19.39	–	–	–	–
$Fe_2O_3^b$	–	–	–	–	–	0.97	0.94	0.87	0.18
MnO	0.72	0.28	0.14	0.39	0.66	–	–	–	–
MgO	19.21	16.11	13.67	27.57	24.59	–	–	–	–
CaO	4.45	18.67	19.99	1.08	1.45	18.37	18.09	18.67	10.68
Na_2O	0.03	0.19	0.39	0.00	0.04	0.96	1.16	1.07	5.30
K_2O	–	–	–	–	–	0.03	0.04	0.00	0.17
Total	100.17	100.09	100.23	100.26	100.62	99.89	99.31	100.42	99.16
Ca%	9.02	37.48	42.31	2.08	2.83	91.20	89.39	90.60	52.17
Mg%	54.16	44.98	40.24	73.84	66.66	–	–	–	–
Fe+Mn%	36.82	17.54	17.45	24.08	30.51	–	–	–	...
K%	–	–	–	–	–	0.18	0.24	0.00	0.99
Na%	–	–	–	–	–	8.62	10.37	9.40	46.85
Mineral	PIG	AU	AU	BR	HY	PL	PL	PL	PL
	GM	PR	PC	PC	PC	PC	PI	PR	PC

	27-7.4	27-1b.2	27-1b.3	16-1.7	16-1.1	16-1.4	27-1a.1	27-1a.2	27-1b.5
SiO_2	55.13	56.29	57.87	55.03	47.45	47.78	49.49	46.66	48.68
TiO_2	–	–	–	–	0.96	0.96	0.78	1.10	0.78
Al_2O_3	28.75	26.95	26.09	27.44	7.84	7.97	7.03	8.59	7.02
Cr_2O_3	–	–	–	–	0.08	0.00	0.00	0.00	0.00
FeO^a	–	–	–	–	12.62	12.26	12.21	12.54	12.61
$Fe_2O_3^b$	0.31	0.28	0.24	0.33	–	–	–	–	–
MnO	–	–	–	–	0.32	0.45	0.65	0.27	0.45
MgO	–	–	–	–	15.52	15.16	16.35	15.55	16.19
CaO	10.73	9.51	8.33	10.13	10.55	10.99	10.06	10.19	10.46
Na_2O	4.92	6.38	6.88	5.42	1.41	1.78	1.50	1.74	1.50
K_2O	0.18	0.19	0.28	0.11	0.15	0.13	0.16	0.25	0.13
Total	99.99	99.57	99.67	98.52	96.90	97.48	98.23	96.89	97.44
K%	1.08	1.06	1.58	0.65	–	–	–	–	–
Na%	44.86	54.25	58.97	48.87	–	–	–	–	–
Ca%	54.06	44.69	39.45	50.48	–	–	–	–	–
Mineral	PL	PL	PL	PL	Mg HBL	ED	Mg HBL	ED	Mg HBL
	PR	PC	PR	GM	PC	PC	PC	PR	PC

PIG = pigeonite; *AU* = augite; *BR* = bronzite; *HY* = hypersthene; *PL* = plagioclase; *Mg HBL* = magnesio-hornblende; *ED* = edenite; *GM* = groundmass crystal; *PR* = phenocryst rim; *PC* = phenocryst core; *PI* = phenocryst intermediate between rim and core. [a] Total Fe as FeO; [b] total Fe as Fe_2O_3. The mineral chemistry data was determined with a Camebax-type automated electron microprobe (Microsonde Ouest, Brest, France). A counting time of six seconds, 15 kV, 10–12 nA, and corrections by the ZAF method were used. For further information concerning operating conditions, see Marcelot et al. (1983)

The old-group plagioclases have more anorthite (An)-rich compositions (andesites An_{45-91}, dacites–An_{39-64}) than those of the young group (andesite–An_{39-55}, dacites–An_{34-58}). Plagioclase from the old- and young-group samples also varies in elements such as K and total Fe (Fig. 7a, b). The old group varies continuously along a negative trend in the graph of K vs. An (Fig. 7a) typical of plagioclase in igneous rocks (Maalöe 1976). Generally, the cores are lower in K and higher in An than the rim- and groundmass-compositions along the old-group trend (Fig. 7a). There is no consistent trend found within the young group on either diagram and there is no clear relationship between the cores and rims of these plagioclases.

Amphiboles. Representative amphibole-phenocryst compositions are given in Table 3. Amphibole is found only in the young group. All are calcic amphiboles of two basic types: magnesio-hornblendes and edenites (see Leake 1978). The amphibole is brown under plain

light and euhedral to subhedral. Occasionally twinning is observed. A few of the amphiboles have opaque rims probably the result of oxidation during extrusion, and several have been completely converted to opaque material. Garcia and Jacobson (1979) call this the "black-type" of amphibole breakdown and relate it to changing volatile conditions during magma eruption.

Oxides. Titanomagnetite exists as phenocryst, microphenocryst, and groundmass phases within both the young and old groups. It is euhedral to anhedral and frequently occurs as inclusions within pyroxenes. All of the oxides analyzed have titanomagnetite compositions that fall within the magnetite to ulvospinel solid-solution series. The old group has higher concentrations of TiO_2 than the young group.

Xenoliths. The mineralogy of the two xenoliths found in the young-group dacites consists of plagioclase, amphibole, titanomagnetite,

and biotite. The xenoliths, just like their host lavas, do not contain pyroxene. The xenoliths contain magnesio-hornblendes and edenite amphiboles similar to those found in the host rocks. Biotite is found in the xenoliths but not in any lavas.

Discussion

Crystal fractionation

Mass-balance calculations (Bryan et. al. 1969) were made to test the effects of crystal-fractionation. Selected trace element modeling results based on these calcula-

tions are given in Table 4 using mineral-partition-coefficients from the literature (Pearce and Norry 1979; Gill 1981; Henderson 1982) and F values from the mass-balance calculations. Several authors have chosen arbitrarily the sum of the squares of the residual (R^2) values below 1.5 (Luhr and Carmichael 1980) or 1.2 (Wyers and Barton 1986) to be indicative of crystal-fractionation, however, R^2 values much greater than about 0.1 suggest that other processes in addition to crystal-fractionation operated within the magmatic system (e.g., assimilation and/or mixing; Defant and Nielsen 1990).

Few of the mass-balance calculations gave acceptable R^2 values (Table 4) with the exception of the old group

Table 4. Selected results of trace element modeling based on least sqaures mass-balance calculations

	P	D	CD	R	Bulk D				
	27-4a-86	17-8-87							
Old group andesite to old-group andesite (SiO_2 range = 58.17–58.50)									
Cr	28	44	19	25	3.14				
Ni	31	30	28	2	1.54				
Rb	20	14	24	−10	0.07	FP	C(%)	F	R^2
Sr	472	499	458	41	1.16				
Y	14	12	16	− 4	0.35	CPX	21.7	0.84	0.15
Zr	68	78	80	− 2	0.06	OPX	11.3		
Nb	7	7	8	− 1	0.16	PL	62.9		
Ba	720	658	836	−178	0.16	MT	4.1		
Th	0.9	1.5	1.1	0.4	0.02				
U	0.4	0.7	0.5	0.2	0.01				
La	8.7	13.2	10.2	3.0	0.11				
Ce	16.6	23.6	19.2	4.4	0.17				
Nd	11.1	13.3	13.1	0.2	0.07				
Sm	2.2	2.2	2.6	− 0.4	0.26				
Eu	0.77	0.80	0.87	− 0.07	0.42				
Yb	1.4	1.5	1.6	− 0.1	0.31				
Lu	0.20	0.26	0.23	0.03	0.25				
	27-5-86	27-2-86							
Old-group andesite to young-group dacite (SiO_2 range = 56.44–68.71)									
Cr	33	10	0.01	10	19.18				
Ni	37	7	13	− 6	3.18	FP	C(%)	F	R^2
Rb	23	22	37	−15	0.05				
Sr	683	772	296	476	2.68	CPX	5.3	0.60	2.27
Y	13	2	5	− 3	2.97	AM	45.2		
Zr	66	71	41	30	1.95	PL	41.8		
Nb	8	7	5	2	2.07	MT	7.8		
Ba	511	752	748	3	0.23				
	27-1b-86	18-2-87							
Young-group andesite to a young-group dacite (SiO_2 range = 58.61–66.80)									
Cr	6	8	7	1	0.75				
Ni	9	4	17	−13	0.01	FP	C(%)	F	R^2
Rb	25	21	46	−25	0.05				
Sr	800	841	252	589	2.84	PL	47.1	0.53	5.45
Y	5	2	1	1	2.98	AM	46.9		
Zr	67	66	36	30	1.97	MT	5.9		
Nb	5	8	2	5	2.06				
Ba	720	578	1149	−572	0.26				

P = parent; D = daughter; CD = calculated daughter; R = residual; Bulk D = bulk distribution coefficient; FP = fractionating phases; $C(\%)$ = percent cumulate; F = weight fraction residual liquid; R^2 = sum of the square of the residuals. The cumulate phases and associated percents, the F values, and R^2 values were determined from mass-balance calculations (Bryan et al. 1969). The F values and cumulate phases were then used to determine CD

where mafic andesites could be related to less-mafic andesites ($R^2 = 0.15$) and dacites could be generated from andesites ($R^2 = 0.55$). For these old-group samples, the mass-balance and trace-element modeling is supported by the mineralogic and petrologic data. For example, the fractionated minerals determined from the mass-balance calculations are consistent with the observed relative phenocryst-proportions in the rocks. In addition, characteristics of the mineral chemistry from the old-group samples exemplify magma-evolution via crystal-fractionation, including: (1) clinopyroxene compositions display a systematic decrease in Ca with an increasing cation Fe/Mg ratio, (2) the K content in plagioclase decreases with increasing anorthite percent (Fig. 7a).

Samples within the young group, however, could not be related by the mass-balance calculations or trace-element modeling (Table 4). While some of the trace-element characteristics (e.g., low Y and HREE) could be accounted for by extreme amphibole-fractionation, the modeling does not support this possibility. In addition, continuous trends among mineral-composition diagrams (e.g., Fig. 7a) do not exist among the young group.

The old and young groups could not be related to each other by a crystal-fractionation model (Table 4). This is not surprising because the two groups are separated by a large time-interval (3.4 Ma) and they have significantly different major-, trace-, and REE-geochem-

istries (Figs. 4, 5, 8). The different phenocryst-assemblages (pyroxenes in the old and amphiboles in the young group) suggest the two groups are not related.

Incompatible elements are generally higher among the dacites compared with the andesites of the old group, consistent with other arc settings (e.g., Lowder and Carmichael 1970; Dixon and Stern 1983). This feature can be explained by the fractionation of phases determined from the mass-balance calculations and those found as phenocrysts (clinopyroxene, orthopyroxene, plagioclase, and titanomagnetite).

The relationship between the incompatible elements of the young group is just the reverse of that expected for fractionation (i.e., a decrease in incompatible elements from the andesite to dacites). Smith and Leeman (1987) found a similar relationship among andesites and dacites from Mount St. Helens and suggested that fractionation of accessory phases could generate the decrease of incompatible elements with differentiation. They suggested that several accessory phases may have been removed simultaneously (e.g., apatite, zircon, monazite, allanite) to explain the "strongly" incompatible-element (e.g., Rb, Ba, Th, U, K) enrichment in the Mount St. Helens dacites relative to andesites. These accessory minerals could not have affected the incompatible elements to any significant extent, because either they are not present in the El Valle samples or they occur
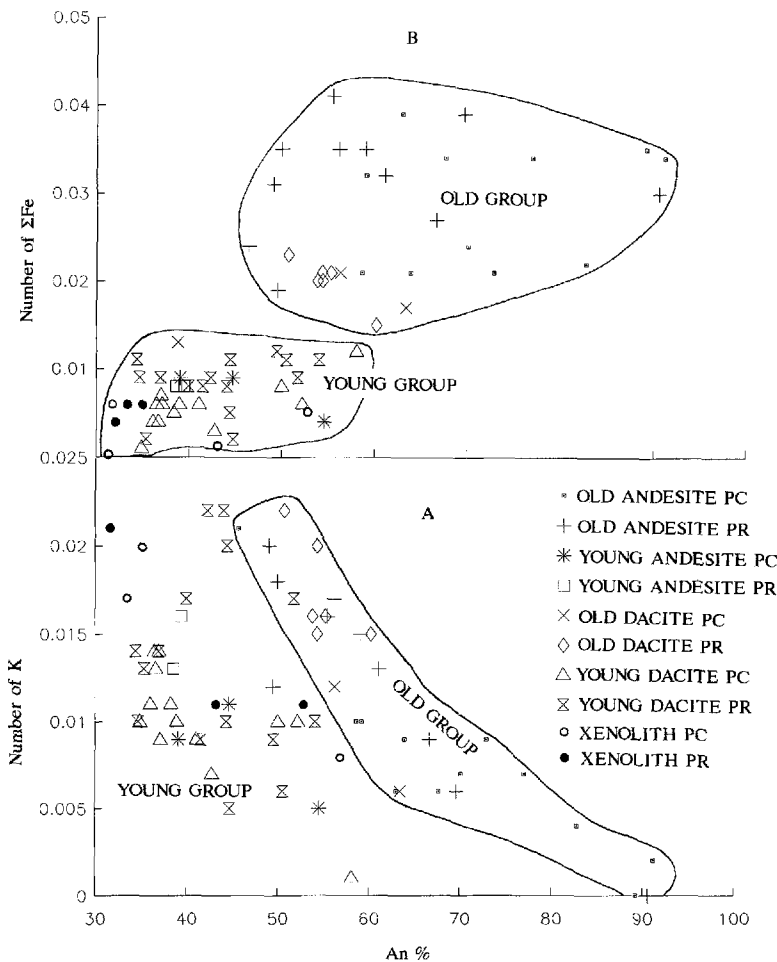

Fig. 7A, B. Anorthite % vs.: A number of K ions in plagioclase per 8 oxygens; B number of total Fe ions in plagioclase per 8 oxygens. PC = core of phenocryst, PR = rim of phenocryst. Groundmass plagioclase phases are included in the PR group
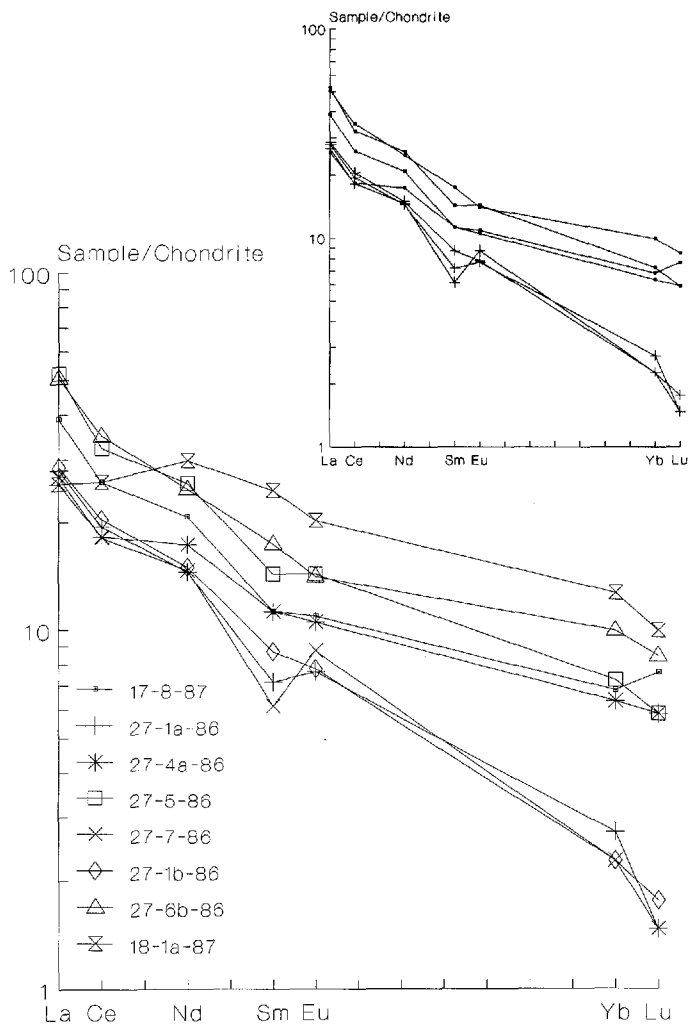
Fig. 8. Chondrite normalized REE diagram. The normalizing values are from Wakita et. al. (1971). The *inset* differentiates the young (*crosses*) and old (*small squares*) groups (xenolith not included in the inset)

to rapid crystal-growth (Hollister and Gancarz 1971; Nakamura 1973) (Fig. 9a), sieve textures in plagioclase that are probably associated with either magma-mixing or assimilation according to the experimental work of Tsuchiyama (1985) (Fig. 9b and c), resorption and embayment along the boundaries of plagioclase (Fig. 9c), and Fe impurities in plagioclase (Fig. 7b). Evidence suggests that many of the phenocrysts have accumulated based on the high anorthite content of some plagioclase phenocrysts, the lower Fe/Mg ratios in the pyroxene phenocrysts compared with whole-rock compositions, and glomeroporphyritic textures (Fig. 9d).

These disequilibrium characteristics are supported by some of the geochemical modeling discussed above, particularly among the young-group samples (e.g., the high R^2 values, large variations in incompatible-element ratios, etc.). The extent of disequilibrium, however, is much more pervasive in the old compared with the young group suggesting that the inability to relate the samples within the young group by mass-balance calculations may not be due completely to complex petrogenetic processes such as assimilation and magma-mixing. We believe complex processes have affected the magmas from both groups to varying degrees. The extent of assimilation of upper crustal material, however, is limited by the relatively low radiogenic Sr and high radiogenic Nd if the crust has distinctly higher $^{87}Sr/^{86}Sr$ and lower $^{143}Nd/^{144}Nd$ than the magmas (Fig. 6).

In summary, we believe that both assimilation/magma-mixing and crystal-fractionation have been involved in the evolution of the magmas. The young-group's geochemical characteristics, however, are not completely explained by these processes. In the following section, we address the influence of the source that may have played an important role in the generation of the El Valle magmas, in particular, the distinct geochemical patterns of the young group.

in very small quantities, a conclusion also reached by Smith and Leeman (1987) for Mount St. Helens.

The unsuccessful modeling of crystal-fractionation for the young group through mass-balance and trace-element modeling, variations in ratios of incompatible elements that are insensitive to crystal-fractionation processes, and the lack of correlations between various elements in plagioclase and amphibole (e.g., Fig. 7a) within the young group may be due to several factors: (1) processes such as assimilation and magma-mixing may have disturbed crystal-fractionation systematics (Defant and Nielsen 1990); and/or (2) the samples may not be cogenetic but derived from separate sources or through different degrees of partial melting.

Assimilation and magma-mixing processes

There is evidence that suggests disequilibrium existed in both the old- and young-group magma chambers during phenocryst-crystallization: oscillatory zoning in both plagioclase and pyroxene phenocrysts perhaps related

Source variations and partial melting

Determination of the origin and petrogenesis of El Valle volcanics is complicated by the absence of basalts throughout the study area. We believe that andesites (and dacites) from the old group have been derived through the differentiation (crystal-fractionation, magma-mixing, and/or assimilation) of more-mafic magmas that originated from partial melting of the mantle wedge. This is based on the following evidence:

1. There is a geochemical similarity between these andesites and other arc andesites generated from basalt-andesite-dacite rhyolite differentiation (e.g., Defant et. al. 1989, in press). In addition, these volcanics are all metaluminous which is typical of basalt-andesite-dacite-rhyolite fractionation suites (Drummond and Defant in press).

2. These andesites and dacites do not meet the criteria established by Gill (1981) and Drummond and Defant (in press) that identify magmas derived from direct partial melting of the subducted lithosphere (or lower crust) (Table 5).
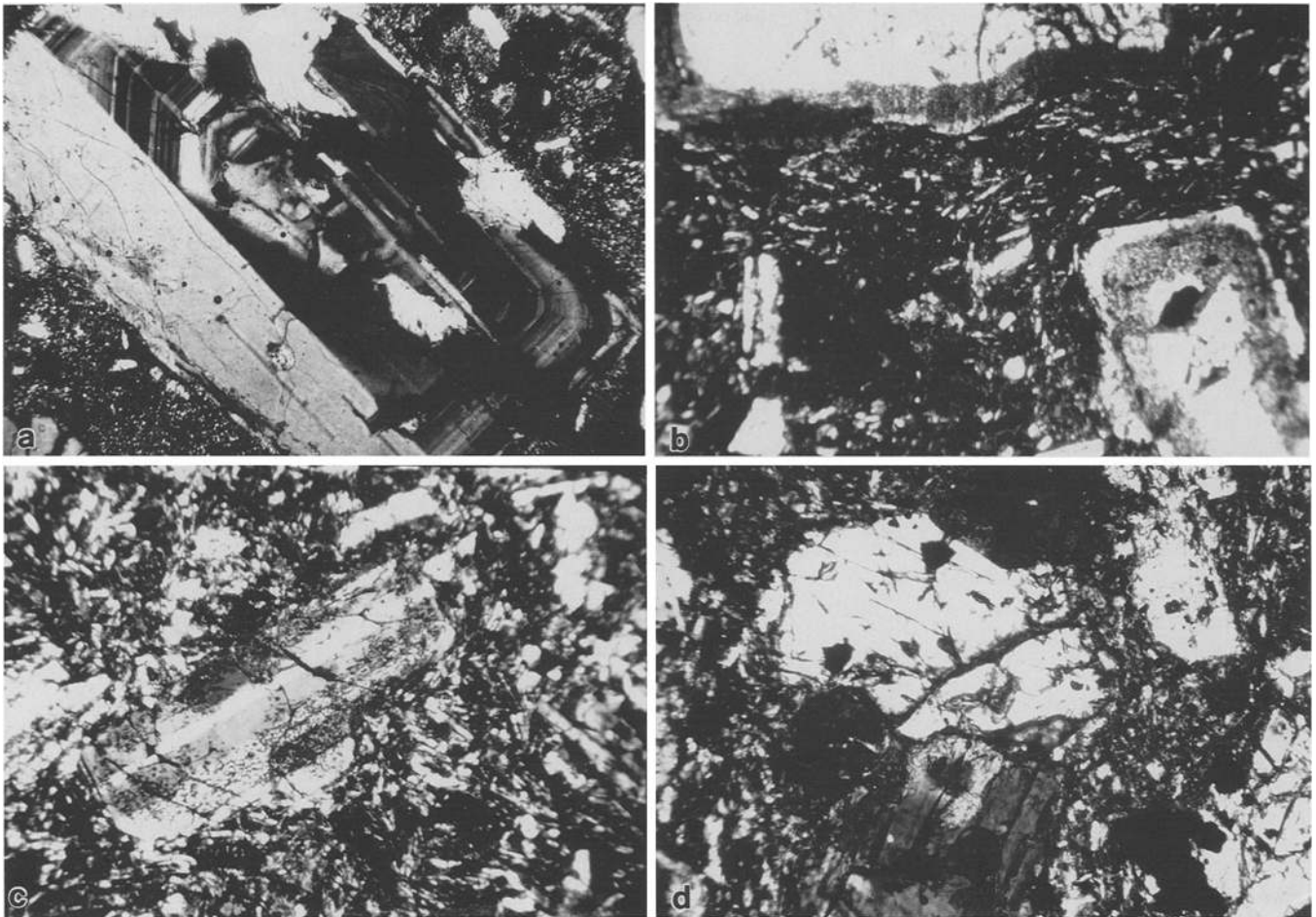
Fig. 9a–d. Photomicrographs: **a** oscillatory zoning in plagioclase – sample 27-7-86, young-group dacite (4 ×); **b** sieve texture in plagioclase – sample 27-4a-86, old-group andesite (4 ×); **c** resorption in plagioclase and sieve textures – sample 17-8-87, old-group andesite (4 ×); **d** glomeroporphyritic texture – sample 27-5-86, old-group andesite (4 ×). Field of view in all micrographs is 2.5 mm

Table 5. Comparison of the geochemical characteristics of magmas derived from the partial melting of the subducted lithosphere (from Gill 1981; Drummond and Defant in press) with those of the young and old groups

Parameter	Characteristic	OA	OD	YA	YD
La/Yb	>20	6.2–11.1 (8.7)	7.8	19.4	15.8–18.2 (17)
Yb	< 1–1.5	1.4–1.6 (1.5)	2.2	0.5	0.5–0.6 (0.55)
Y	<15–18	12–14 (13)	20–29 (24)	5	2–4 (2.5)
Sr/Y	>40	34–53 (43)	13–18 (15)	160	176–420 (328)
Al$_2$O$_3$	>15%	16.7–17.6 (17.1)	15.5–15.6 (15.5)	17.5	17.2–17.6 (17.5)

The average of the range is given in parentheses. OA = Old-group andesites; OD = Old-group dacites; YA = Young-group andesite; YD = Young-group dacites

3. The samples low-MgO concentrations (and other geochemical parameters) rule out a direct derivation from the mantle wedge.

Several of the geochemical features of the young group are compared with those of the old group and those expected in magmas derived from partial melting of the lithosphere (Table 5) as noted by Gill (1981) and Drummond and Defant (in press). The young group has higher La/Yb and Sr/Y ratios and lower Yb (Fig. 8) and Y concentrations (Fig. 5) than the old group. These characteristics can be explained by the partial melting of a source with residual garnet and amphibole (e.g., low Y and Yb) (amphibolite to eclogite).

Defant and Drummond (in press) found that Cenozoic arc andesites, dacites, and rhyolites (ADR) with similar geochemical signatures to the El Valle young group are associated with the subduction of young and hot oceanic crust. They suggested that when relatively hot crust is subducted partial melting of the slab can occur. They termed the rocks produced in this manner
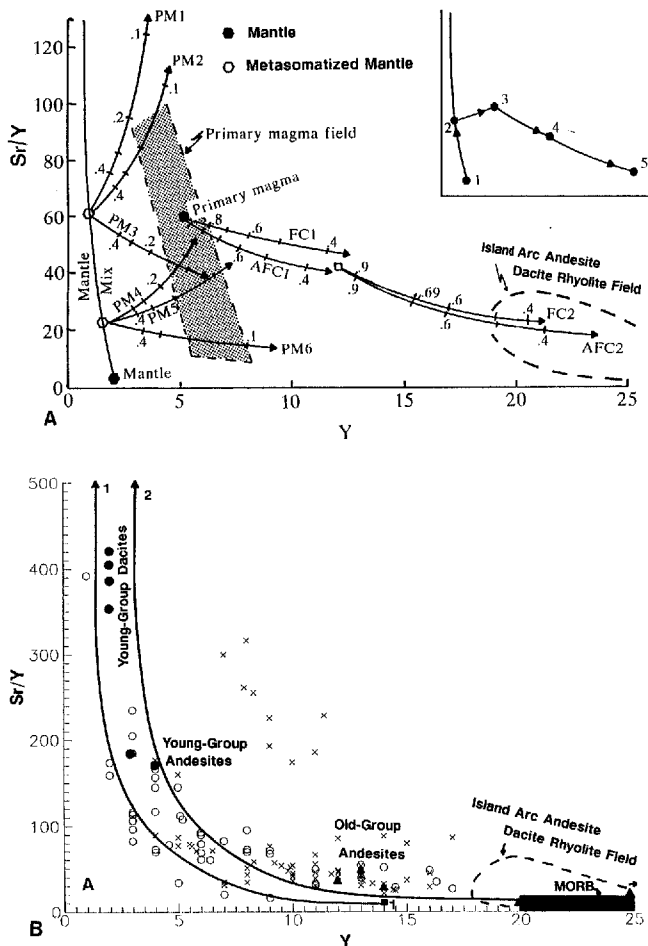
Fig. 10A, B. Graph of Sr/Y vs. Y. **A** The diagram and *inset* depict a petrogenetic model where the old-group samples and ADR island-arc suites, in general, can be derived. The mantle composition (*# 1, inset*) and the composition of lithosphere-dehydration fluids (projects off the graph toward high Sr/Y and low Y) (from Hole et. al. 1984). A mixing curve ("mantle-mix") between these two end-members represents potential metasomatized-mantle compositions. Two compositions that approach realistic metasomatized-mantle compositions have been chosen along the *curve* (*open hexagons* and *#2, inset*). The *curves* labeled PM1 through PM6 are partial-melting models starting with the two potential mantle compositions (Pearce and Norry 1979) shown as *open hexagons:* curve *PM1* source=60% OL, 20% OPX, 20% CPX; curve *PM2* source=40% OL, 30% CPX, 30% OPX; curve *PM3* source 60% OL, 20% OPX, 10% CPX, 10% PL (source composition – Sr = 60.91, Y=1), curves *PM4, PM5, PM6* have the same source mineral-percentages as PM1, PM2, PM3, respectively (source composition – Sr=33.65, Y=1.5). The primary magma-field is an estimation based on realistic melts derived from the range of "reasonable" potential mantle-compositions and mineral-percentages. The primary magma (*# 3, inset*) has been chosen because of its central location within the primary magma-field (Sr=300, Y=5). Curve *FC1* is a Raleigh crystal-fractionation curve generated from the primary magma-composition (fractionating phases=30% OL, 30% CPX, 30% PL, 10% MGT (magnetite)) and *curve AFC1* is generated from the same magma and fractionating phases using the equations of DePaolo (1981), an r value of 0.2, and an assimilant from Glikson (1976). These equations attempt to show that the old-group andesites (*#4, inset*) can be generated from crystal fractionation and/or AFC processes from a primary magma and can evolve to the dacite compositions (*#5, inset*). The crystal fractionation (*FC2*) and AFC (*AFC2*) trends were derived using the same equations and parameters as those used to derive curves FC1 and AFC1 except that the fractionating phases chosen were 9.5% CPX, 28.8% OPX, 59% PL, 2.6% MGT – phases common in

adakites after rocks with similar geochemical signatures first described from Adak Island (Kay 1978).

Defant and Drummond (in press) found that a diagram of Sr/Y vs. Y is sensitive in discriminating between slab-derived and mantle-wedge-derived magmas. The derivation of "normal" island-arc ADR volcanics through partial melting of the mantle wedge and subsequent differentiation (AFC, magma mixing, fractional crystallization) is modeled in Figure 10a. The model shows that basalts differentiate toward higher Y and lower Sr/Y values (note the ADR island-arc field with >18 ppm Y values in Fig. 10a). In contrast, higher Sr/Y and lower Y values are generated from the partial melting of metamorphosed MORB (mid-ocean-ridge basalt) to produce adakites than the normal island arc magmas (Fig. 10b). Included on Figure 10b are high-Al Archean trondhjemites, tonalites, and dacites (TTD) that are believed to be derived from the partial melting of subducted oceanic crust (Jahn et. al. 1981; Martin 1986, 1987; Drummond and Defant in press).

The El Valle young group falls within the adakite field and the old-group dacites fall into the normal island-arc field (Fig. 10b). The old-group andesites fall out of the normal-arc field but do not have other characteristics of adakites (e.g., low La/Yb ratios – Fig. 8).

In conclusion, although crystal-fractionation (particularly amphibole-fractionation) and/or assimilation can account for some of the variability among the data, these processes cannot fully explain the young-group trend (Fig. 10b). We suggest that the young-group trend is the result of a combinaton of variable degrees of partial melting, source-composition, amphibole-fractionation, and AFC-processes.

We have suggested that the young group has been derived from the subducted lithosphere but there are alternative sources: primarily the lower crust and garnet peridotite in the upper mantle. There is no a priori reason to believe that the source is the lower crust. Granulite-facies rocks in the lower crust commonly have Sr and Nd isotopic ratios that fall below the mantle array (e.g., Downes and Leyreloup 1986; Faure 1986). Magmas generated from such a source likely would have these distinctive isotopic ratios which are absent in the young-group volcanics although van Calsteren et. al. (1986) note that these lower-crust geochemical features are not ubiquitous. Magmas derived from the partial melting of a plagioclase-rich granulite or amphibolite would produce negative Eu anomalies whereas lithosphere converted to eclogite during subduction would be absent of plagioclase and would produce magmas with small or absent Eu anomalies. The young-group samples do not have distinctive Eu anomalies (Fig. 8). Hydrous partial melting of a garnet peridotite (upper

these evolved rocks. Intermediate mineral partition-coefficients were also used. **B** Adakites (*x*) and Archean high-Al TTD (*open circles*) thought to be derived from subducted oceanic crust (after Defant and Drummond in press). The MORB field is shown and partial-melting curves from MORB and Archean amphibolite (*squares*) are superimposed on the diagram. El Valle young group (*filled circles*) and old group (*filled triangles*) are included on the diagram

mantle) would generate high-Mg andesites (11–20-wt% MgO – Jenner 1981; Kushiro 1972; Green 1973, 1976) but the young-group andesite has a MgO value of 3.59 wt%.

Synthesis

In the Archean, the higher heat-content of the Earth probably generated smaller plates (and therefore more numerous plates) which moved more quickly and subducted faster than the plates of today (e.g., Martin 1986). This apparently led to the partial melting of the subducted lithosphere rather than the mantle wedge, generating the vast Archean TTD-craton complexes of the world. A few areas of the world, however, may be undergoing lithosphere melting because of the high heat-content of the subducted lithosphere (one example is where mid-ocean ridges exist in close proximity to the trench – e.g., the Austral Andes, Stern et. al. 1984).

De Boer et. al. (1988) have noted that the Panama basin has extremely high heat-flow values comparable to some MOR. It appears that the lithosphere is subducted at elevated temperatures compared to other island-arc systems. The contrast between the origins of the old (mantle-derived) and young (slab-derived) group suggests that the conditions of subduction may have changed during the 3.4-million-year hiatus.

Two hypotheses, in no particular order, are presented to explain the eruption at the same locality of volcanics which have been derived through different processes. The first is based on the work presented by Cross and Pilger (1982). The production of early mantle-derived volcanics from a depth of approximately 120 km followed by relatively shallow-level (75–85 km) lithosphere-derived dacites at the same or nearby volcanic conduit may be due to differing absolute plate-motion through time. Slow absolute upper-plate-motion toward the trench produces a steeply dipping subduction zone whereas rapid absolute upper-plate-motion generates a shallow-inclined subduction zone.

The second hypothesis involves Vlaar's (1989) suggestion that the behavior of the subducted lithosphere depends on its temperature (and therefore its age). The subduction of young and relatively hot lithosphere would cause more buoyancy and result in the subducted lithosphere remaining "afloat" at shallow depths as compared with the subduction of an older lithospheric plate. We surmise that perhaps the early subduction of a cold lithosphere (between 5 and 10 Ma) below Panama resulted in normal-arc magmatism (i.e., derivation of basaltic magmas within the mantle wedge at deeper levels, e.g., 120 km, which differentiated to andesites and dacites as the magmas rose to the surface or perhaps at the mantle-crust boundary). The products of these processes were the old group. In contrast, as the lithosphere became hotter, relatively speaking, the lithosphere rose and eventually partial melting occurred generating the young-group andesite and dacites. Based on experimental work, this process should take place at shallower depths than the mantle-melting (e.g., 75–85 km – see Drummond and Defant in press). Due to

the fact that the lithosphere rose as a result of the higher temperatures, the old and young groups were erupted at the same locality (El Valle – the old group from deeper and the young group from shallower depths). At this time, we cannot rule out either of these proposed hypotheses.

References

Adamek S, Frohlich C, Pennington WD (1988) Seismicity of the Caribbean-Nazca boundary: Constraints on microplate tectonics of the Panama region. J Geophys Res 93:2053–2075

Bowin CO (1976) The Caribbean: gravity field and plate tectonics. Geol Soc Am Spec Pap 169

Bryan WB, Finger LW, Chayes F (1969) Estimating proportions in petrographic mixing equations by least-squares approximation. Science 163:926–927

Clark LF, Defant MJ, Stewart RH, Drummond MS, Mukasa SB (1988) Geology and petrogenesis of El Valle volcano, Panama. Am Geophys Union EOS 69:1491

Clark LF (1989) The geology, geochemistry, and petrogenesis of El Valle volcano (Panama). Masters Thesis, University of South Florida, USA, 136 p

Cross TA, Pilger RH (1982) Controls of subduction geometry, location of magmatics arcs, and tectonics of arc and back-arc regions. Geol Soc Am Bull 93:545–562

de Boer JZ, Defant MJ, Stewart RH, Restrepo JF, Clark LF (1988) Quaternary calc-alkaline volcanism in western Panama: regional variation and implication for plate tectonic framework. J South Am Earth Sci 1:275–293

Defant MJ, Drummond MS (in press) Derivation of some modern arc magmas by melting of young subducted lithosphere. Nature

Defant MJ, Nielsen RL (1990) Interpretation of open system petrogenetic processes: Phase equilibria constraints on magma evolution. Geochim Cosmochim Acta 54:87–102

Defant MJ, Restrepo JF, Stewart RH, de Boer JZ (1987) Pleistocene to Recent volcanism in western Panama: a geochemical and tectonic investigation (abstract). Am Geophys Union EOS 68:1526

Defant MJ, Jacques D, Maury RC, de Boer JZ (1989) Geochemistry of the Luzon arc, Philippines. Geol Soc Am Bull 101:663–672

Defant MJ, Maury RC, Ripley EM, Feigenson MD, Jacques D (in press) An example of island arc petrogenesis: Geochemistry and petrology of the southern Luzon arc, Philippines. J Petrol

DePaolo DJ (1981) Trace element and isotopic effects of combined wallrock assimilation and fractional crystallization. Earth Planet Sci Lett 53:189–202

Dixon TH, Stern RJ (1983) Petrology, chemistry, and isotopic composition of submarine volcanoes in the southern Mariana arc. Geol Soc Am Bull 94:1159–1172

Downes H, Leyreloup A (1986) Granulitic xenoliths from the French massif central: Petrology, Sr and Nd isotopc systematics and model age estimates. In Dawson JB, Carswell DA, Hall J, Wedepohl KH (eds) The nature of the lower continental crust. Geol Soc Spec Publ 24:319–330

324

Drummond MS, Defant MJ (in press) A model for trondhjemite-tonalite-dacite genesis and crustal growth via slab melting. Archean to modern comparisons. J Geophys Res

Epp D, Grim PJ, Langseth MG (1970) Heat flow in the Caribbean and Gulf of Mexico. J Geophys Res 75:5655–5661

Faure G (1986) Principles of isotope geochemistry. John Wiley and Sons, New York

Feigenson MD, Carr MJ (1986) Positively correlated Nd and Sr isotope ratios of lavas from the Central American volcanic front. Geology 14:79–82

Garcia MO, Jacobson SS (1979) Crystal clots, amphibole fractionation and the evolution of calc-alkaline magmas. Contrib Mineral Petrol 69:319–327

Gill JB (1981) Orogenic andesites and plate tectonics. New York, Springer-Verlag

Glickson AY (1976) Trace element geochemistry and origin of early Precambrian acid igneous series, Barberton Mountain Land, Transvaal. Geochim Cosmochim Acta 40:1261–1280

Green DH (1973) Experimental melting studies on a model upper mantle composition at high pressure under water-saturated and water under-satured conditions. Earth Planet Sci Lett 19:37–53

Green DH (1976) Experimental testing of "equilibrium"partial melting of peridotite under water-saturated, high pressure conditions. Can Mineral 14:255–268

Heil DJ (1988) Response on an accretionary prism to transform ridge collision south of Panama. Master Thesis, University of California, Santa Cruz, USA

Henderson P (1982) Inorganic Geochemistry. Pergamon Press, Oxford, England

Hole MJ, Saunders AD, Marriner GF, Tarney J (1984) Subduction of pelagic sediments: implications for the origin of Ce-anomalous basalts from the Mariana Islands. J Geol Soc London 141:453–472

Hollister LS, Gancarz AJ (1971) Compositional sector-zoning in clinopyroxene from the Narce area, Italy. Am Mineral 56:959–979

IRHE (1985) Estudio de prefactibilidad avanzada de la region del Valle de Anton y Tonosi. Instituto de Recursos Hydraulicos y Electrificacion, Informe del Convenio IRHE-BID-OLADE

Jahn BM, Glikson AY, Peucat JJ, Hickman AH (1981) REE geochemistry and isotopic data of Archean silic volcanics and granitoids from the Pilbara Block, Western Australia: implications for early crustal evolution. Geochim Cosmochim Acta 45:1633–1652

Jenner GA (1981) Geochemistry of high-Mg andesites from Cape Vogel, Papua New Guinea. Chem Geol 33:307–332

Jordon TH (1975) The present-day motions of the Caribbean plate. J Geophys Res 80:4433–4439

Kay RW (1978) Aleutian magnesian andesites: melts from subducted ocean crust. J Volcanol Geothermal Res 4:117–132

Kushiro I (1972) Effect of water on the composition of magmas formed at high pressures. J Petrol 13:311–334

Leake BE (1978) Nomenclature of amphiboles. Am Mineral 63:1023–1053

Lonsdale P, Klitgord KD (1978) Structure and tectonic history of the eastern Panama Basin. Geol Soc Am Bull 89:981–999

Lowder GG, Carmichael ISE (1970) The volcanoes and caldera of Talasea, New Britain: Geology and petrology. Geol Soc Am Bull 81:17–38

Luhr JF, Carmichael SE (1980) The Colima volcanic complex, Mexico. Contrib Mineral Petrol 71:343–372

Maalöe S (1976) The zoned plagioclase of the Skaergaard intrusion, East Greenland. J Petrol 17:398–418

Marcelot G, Maury RC, Lefevre C (1983) Mineralogy of Erromango lavas (New Hebrides): Evidence of an early stage of fractionation in island arc basalts. Lithos 16:135–151

Martin H (1986) Effect of steeper Archean geothermal gradient on geochemistry of subduction-zone magmas. Geology 14:753–756

Martin H (1987) Petrogenesis of Archean trondhjemites, tonalites, and granodiorites from eastern Finland: major and trace element geochemistry. J Petrol 28:921–953

Munoz AV (1988) Tectonic patterns of the Panama block deduced from seismicity, gravitational data and earthquake mechanisms: implications to the seismic hazard. Tectonophysics 154:253–267

Nakamura Y (1973) Origin of sector-zoning of igneous clinopyroxenes. Am Mineral 58:986–990

Okaya DA, Ben-Avraham Z (1987) Structure of the continental margins of southwestern Panama. Geol Soc Am Bull 99:792–802

Pearce JA, Norry MJ (1979) Petrogenetic implications of Ti, Zr, Y, and Nb variations in volcanic rocks. Contrib Mineral Petrol 69:33–47

Peccerillo A, Taylor SR (1976) Geochemistry of Eocene calc-alkaline volcanic rocks from the Kastamonu area, Northern Turkey. Contrib Mineral Petrol 58:63–81

Restrepo JF (1987) A geochemical investigation of Pleistocene to Recent calc-alkaline volcanism in western Panama. Masters Thesis, University of South Florida, Tampa, Fla. USA, 103 p

Richerson PM (1990) Petrogenesis of La Yeguada volcanic complex, western Panama, via both differentiation and slab melting. Masters Thesis, University of South Florida, USA, 133 p

Silver EA, Reed DL, Tagudin JE, Heil DJ (1990) Implications of the north and south Panama thrust belts for the origin of the Panama orocline. Tectonics 9:261–281

Smith DR, Leeman WP (1987) Petrogenesis of Mount St. Helens dacitic magmas. J Geophys Res 92:10313–10334

Steiger RH, Jager E (1977) Subcommission on geochronology: Convention on the use of decay constants in geo- and cosmochronology. Earth Planet Sci Lett 36:359–362

Stern CR, Futa K, Muehlenbachs K (1984) Isotope and trace element data for orogenic andesites from the Austral Andes. In: Harmon RS, Barreiro BA (eds) Andean magmatism – chemical and isotopic constraints. Shiva Publications, Cheshire, pp 31–46

Tsuchiyama A (1985) Dissolution kinetics of plagioclase in the melt of the system diopside-albite-anorthite, and origin of dusty plagioclase in andesites. Contrib Mineral Petrol 89:1–16

van Calsteren PWC, Harris NBW, Hawkesworth CJ, Menzies MA, Rogers NW (1986) Xenoliths from southern Africa: Perspective on the lower on the lower crust. In: Dawson JB, Carswell DA, Hall J, Wedepohl KH (eds) The nature of the lower continental crust. Geol Soc Spec Publ 24:351–362

Vlaar NJ (1986) Subduction of young lithosphere: lithospheric doubling, a possible scenario. In: Hart SR, Gulen L (eds) Crust mantle recycling at convergence zones. Kluwer Academic Publishers, Dordrecht, pp 65–74

Von Herzen RP, Anderson RN (1972) Implications of heat flow and bottom water temperature in the eastern equitorial Pacific. J Geophys Res 26:4–8

Wakita H, Rey P, Schmitt RA (1971) Abundances of the 14 rare earth elements and 12 other trace elements in Apollo 12 samples: five igneous and one breccia rocks and four soils. Proc 2nd Lunar Sci Conf, pp 1319–1329

White WM, Hofmann AW (1982) Sr and Nd isotope geochemistry of oceanic basalts and mantle evolution. Nature 296:821–825

White WM, Patchett J (1984) Hf-Nd-Sr isotopes and incompatible element abundances in island arcs: implications for magma origins and crust-mantle evolution. Earth Planet Sci Lett 67:167–185

Wyers GP, Barton M (1986) Petrology and evolution of transitional alkaline – sub alkaline lavas from Patmos (Dodecanesos), Greece: evidence for fractional crystallization, magma mixing and assimilation. Contrib Mineral Petrol 79:297–311

Editorial responsibility: T. Grove